

# 非圆形微通道热沉的流动换热特性数值模拟

肖春梅, 陈永平, 施明恒, 杨迎春  
(东南大学 能源与环境学院, 江苏 南京 210096)

**摘 要:**建立了非圆形硅微通道内单相流动和换热过程的三维模型,并分别对三角形、矩形和梯形微通道中流动换热进行了数值模拟。研究发现,截面平均努塞尔数在通道入口处数值最大,然后沿流体流动方向急剧减小,直至流动充分发展时趋于恒定。固体和流体温度沿流动方向近似线性升高。换热面壁温仅沿流动方向升高,在垂直于流动方向,温度则基本保持均衡;雷诺数对微通道的流动与换热特性存在着较大的影响,雷诺数越大,其对应的努塞尔数也越大。对 3 种微通道的热经济性分析比较发现,三角形通道的热有效性最高。

**关 键 词:**微通道;数值模拟;传热

中图分类号:TK124 文献标识码:A

## 符号说明

$A_c$ —通道横截面积/ $m^2$ ;	$u, v, w$ — $x, y, z$ 方向上的速度/ $m \cdot s^{-1}$ ;
$c_p$ —比热容/ $kJ \cdot (kg \cdot K)^{-1}$ ;	$\mu$ —动力粘度/ $Pa \cdot s$ ;
$d_h$ —微通道的水力直径/ $m$ ;	$\nu$ —运动黏度/ $m^2 \cdot s^{-1}$ ;
$k$ —导热系数/ $W \cdot (m \cdot K)^{-1}$ ;	$\rho$ —密度/ $kg \cdot m^{-3}$ ;
$P$ —泵功/ $W$ ;	$f$ —流体;
$p$ —压强/ $Pa$ ;	$in$ —入口;
$Q$ —换热量/ $W$ ;	$\Gamma$ —固液界面;
$q_v$ —体积流量/ $m^3 \cdot s^{-1}$ ;	$s$ —固体
$q''$ —热流密度/ $W \cdot m^{-2}$ ;	
$T$ —温度/ $K$ ;	

## 引 言

自从 Tuckerman 和 Pease 提出 MEMS 微通道散热器以来<sup>[1]</sup>,各国学者在该领域开展了广泛的研究<sup>[2~5]</sup>。在微通道内液体流动的理论研究中,通常认为 Navier-Stokes 方程在 30  $\mu m$  以上尺度仍可适用<sup>[6]</sup>。由此,Qu 等人对矩形截面微通道换热器中的传热过程进行了数值模拟<sup>[7]</sup>,Li 等人则数值研究了梯形硅微通道中层流流动换热特性<sup>[8]</sup>。

尽管目前在微通道单相流动与换热领域已开展了较多的研究,但是由于过程的复杂性,很多问题仍不够明了,尤其是通道截面形状对于微通道流动换热特性影响的研究更是非常缺乏。为此,本文对三

角形、矩形和梯形等非圆形微通道内的强制对流换热过程进行了三维数值模拟研究,给出了各类截面微通道热沉内的流动和换热特性参数,并对 3 种通道的热经济性进行了分析比较。

## 1 数学物理模型

研究的微通道热沉系统的结构如图 1(a) 所示,主要由硅基、导热系数很小的耐热玻璃组成,冷却工质为去离子水。硅片上等距布有平行通道,如图 1(b)所示,其具体尺寸如表 1 所示。

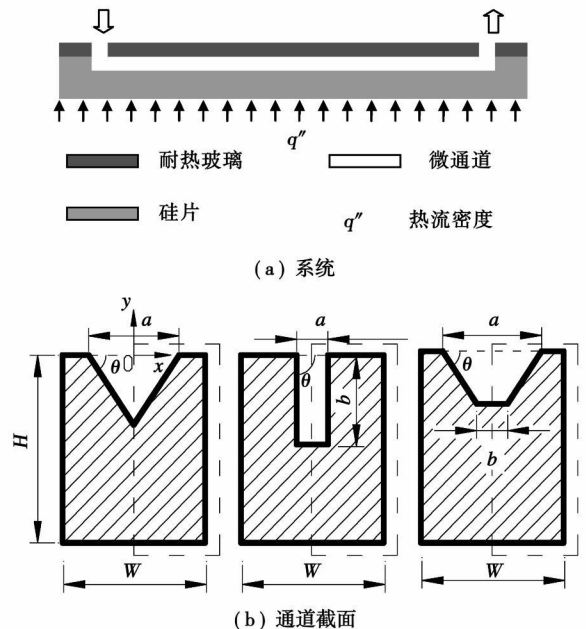


图 1 微通道热沉结构图

表 1 微通道热沉单元尺寸

	$a/\mu m$	$b/\mu m$	$\theta/(^\circ)$	$H/mm$	$W/mm$	$L/mm$
三角形	129.6	—	54.7	0.5	0.3	40
矩形	40	200	90	0.5	0.3	40
梯形	158	62	54.7	0.5	0.3	40

收稿日期: 2007-12-27; 修订日期: 2008-05-04

基金项目: 江苏省自然科学基金资助项目(BK2008309); 博士学科点专项科研基金资助项目(20070286072)

作者简介: 肖春梅(1982—)女,山东威海人,东南大学硕士研究生。

1.1 控制方程和边界条件

在控制单元体内, 热量通过硅的导热传导到微通道壁面, 再经过对流换热由冷却工质将热量带走。为简化分析, 假设: (1) 忽略重力影响; (2) 流动和传热过程是稳态的; (3) 层流流动; (4) 固体和液体热物性不变。这样, 流体的连续性方程、动量方程和能量方程分别为:

$$\nabla V=0 \tag{1}$$

$$\rho_f (V \cdot \nabla V) = -\nabla p + \mu_f \nabla^2 V \tag{2}$$

$$\rho_f c_{p,f} (V \cdot \nabla T) = k_f \nabla^2 T \tag{3}$$

固体内的导热方程为:

$$k_s \nabla^2 T=0 \tag{4}$$

对于流体, 在进口处的速度、温度边界条件为:

$$\text{当 } z=0, w=w_{in}, u=0, v=0, T=T_{in} \tag{5}$$

在出口处达到充分发展, 边界条件为:

$$\text{当 } z=L, \frac{\partial u}{\partial z}=0, \frac{\partial v}{\partial z}=0, \frac{\partial w}{\partial z}=0, \frac{\partial T}{\partial z}=0 \tag{6}$$

对于固体, 在控制单元底部为恒热流边界条件,

$$\text{当 } y=-H, -k_s \frac{\partial T}{\partial y}=q'' \tag{7}$$

在控制单元体上表面, 为绝热边界条件,

$$\text{当 } y=0, -k_s \frac{\partial T}{\partial y}=0 \tag{8}$$

在控制单元体侧面, 由结构的对称性,

$$\text{当 } x=\pm W/2, -k_s \frac{\partial T}{\partial x}=0 \tag{9}$$

在控制单元体内, 导热和对流通过固液界面耦合。因此, 固液界面的边界条件为:

$$T_s|_{\Gamma}=T_f|_{\Gamma} \tag{10}$$

$$-k_s \left. \frac{\partial T_s}{\partial n} \right|_{\Gamma} = -k_f \left. \frac{\partial T_f}{\partial n} \right|_{\Gamma} \tag{11}$$

$$u|_{\Gamma}=0, v|_{\Gamma}=0, w|_{\Gamma}=0 \tag{12}$$

1.2 求解方法

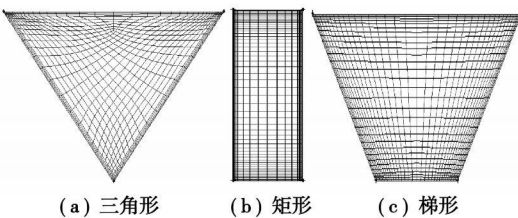


图 2 网格划分示意图

采用 SIMPLE 算法和有限差分法求解流体和固体的控制微分方程。在通道入口截面的边界层和通道角点处进行网格加密, 以便考虑流动和传热的入口效应和边界层效应, 如图 2 所示。方程经离散后, 由 Gauss-Sedial 方法迭代求解, 当相对误差小于  $10^{-6}$

时, 认为迭代收敛。

2 模拟结果与讨论

2.1 传热和流动特性

表 2 数值计算中所用传热参数

$w_{in}$ /m <sup>3</sup> s <sup>-1</sup>	$T_{in}$ /°C	$q''$ /W <sup>2</sup> cm <sup>-2</sup>	$k_f$ /W <sup>2</sup> (m <sup>3</sup> °C) <sup>-1</sup>	$k_s$ /W <sup>2</sup> (m <sup>3</sup> °C) <sup>-1</sup>
3	20	30	0.61	157

数值计算中所用到的参数如表 2 所示。图 3 为表 2 所示工况下, 计算得到的 3 种不同截面微通道中截面平均  $Nu$  数沿轴向的变化趋势, 图 4 为不同  $Re$  数下梯形通道中  $Nu$  数计算值与实验数据的对照图<sup>[6]</sup>。 $Nu$  数定义如下:

$$Nu = \frac{q'' d_h}{k_f (T_{\Gamma,m} - T_m)} \tag{13}$$

式中:  $T_{\Gamma,m}$ —固液界面的平均温度。

$$T_{\Gamma,m} = \frac{1}{\Gamma} \int_{\Gamma} T d\Gamma \tag{14}$$

式中:  $T_m$ —流体的截面平均温度。

$$T_m = \frac{\int_{A_c} w T dA_c}{\int_{A_c} w dA_c} \tag{15}$$

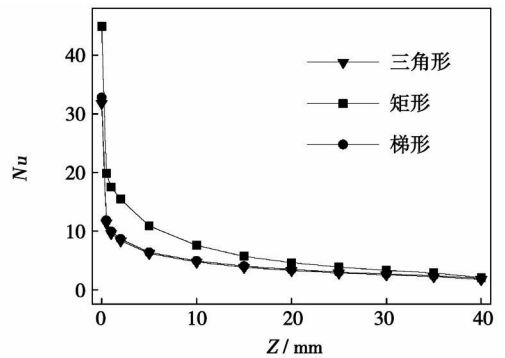


图 3 截面平均  $Nu$  数沿轴向的变化趋势

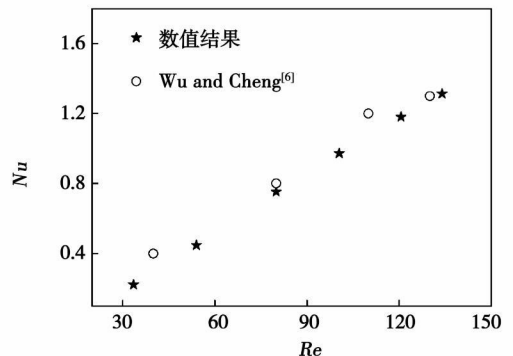


图 4 数值计算  $Nu$  数与实验数据的对照<sup>[6]</sup>

从图 3 中可以看出, 三类通道中,  $Nu$  数在通道

入口处皆出现最大值, 然后急剧减小, 直至趋于稳定; 3 种通道中, 矩形的截面平均  $Nu$  数最高。从图 4 可知, 在很宽的  $Re$  数范围内, 数值计算得到的  $Nu$  数都可以与实验数据很好的吻合。从而证明了本文所采用的模型是合理的。

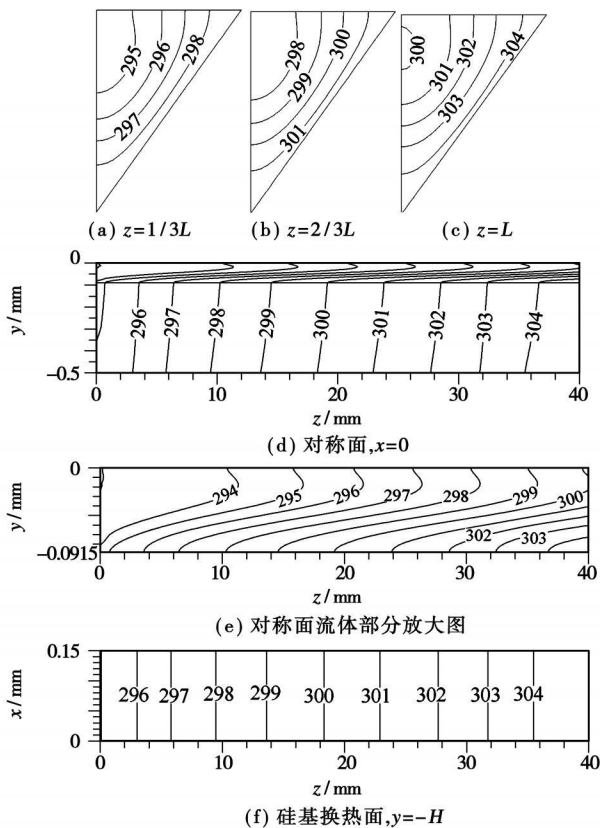


图 5 三角形硅微通道中各截面温度分布

图 5 ~ 图 7 分别是在表 2 工况下, 三类微通道中, 沿流程的 3 个特征横截面 ( $z = 1/3L, z = 2/3L, z = L$ )、中心对称面 ( $x = 0$ ) 和热沉的下表面 (换热面,  $y = -H$ ) 的温度分布图。从图 5 ~ 图 7 中 (a) ~ (c) 可以看出, 三类通道中流体的中心位置温度皆较低, 而外侧温度较高; 从 (d) ~ (f) 可以看出, 在三角形和梯形通道中, 上层流体较下层流体会有一定的温度滞后, 最低温度出现在通道上中层; 而在矩形通道中, 尽管上层流体较下层流体仍有温度滞后, 但是滞后度已大为减小, 最低温度已接近通道中心层。这说明, 通道形状对于流体温度场分布存在着很大的影响。三类通道中, 固体温度皆沿流动方向逐渐升高, 在入口处温度梯度较大。由于恒热流边界条件的存在, 在流动充分发展段, 对称面硅基内的等温线呈稍微倾斜的平行线, 而在硅基换热面, 其等温线与  $x$  轴近似平行, 且基本等距, 这就表明微通道热沉系统换热面壁温沿流动方向近似线性升高, 在垂直于

流动方向, 温度保持均衡。

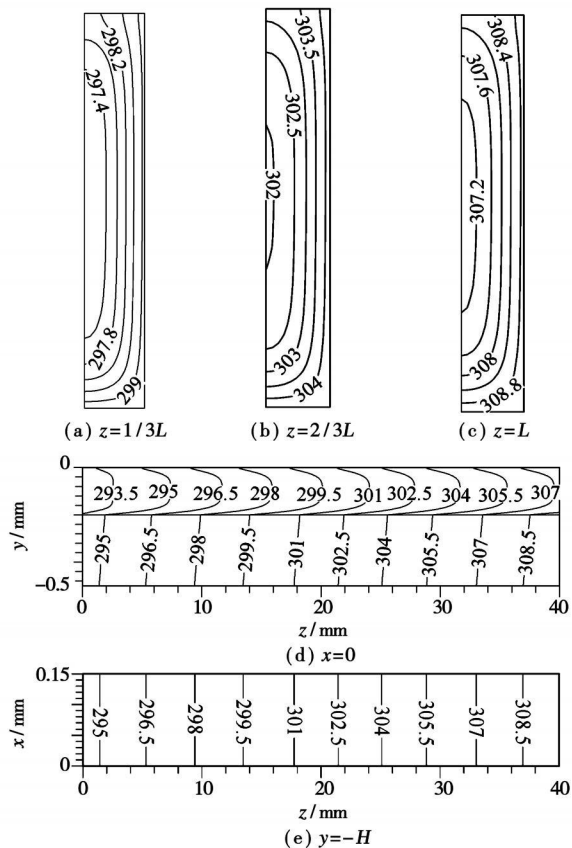


图 6 矩形硅微通道中各截面温度分布

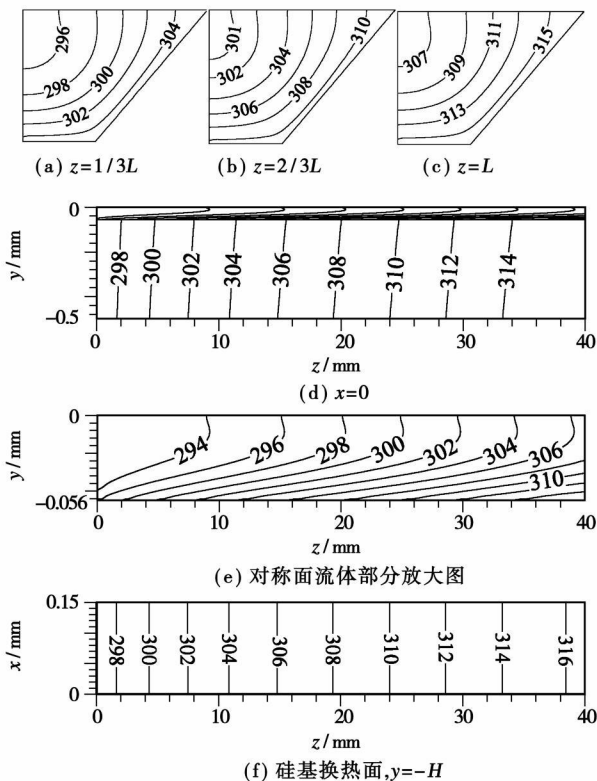


图 7 梯形硅微通道中各截面温度分布

### 2.2 雷诺数的影响

图 8 给出了不同截面微通道中截面平均努塞尔数沿轴向的变化趋势。由图可见, 不管何类形状通道, 对于给定的某个轴向位置  $z$ , 平均努塞尔数皆随雷诺数的增加而增加。这与 Qu 等人的结论一致<sup>[7]</sup>。图 9 和图 10 分别为不同截面形状微通道中流体截面平均温度和硅基下表面(换热面)温度沿轴向的变化趋势。由图可知, 流体和固体温度沿流动方向近似线性变化, 且随着雷诺数的增加, 微通道进出口温差显著减小。

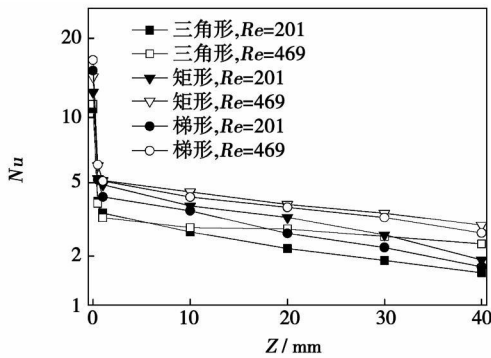


图 8 截面平均  $Nu$  数随  $Re$  的变化

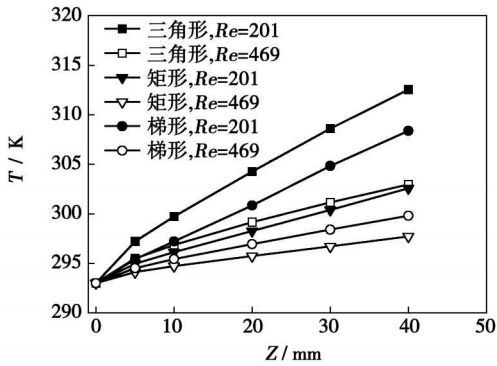


图 9 流体温度沿轴向随雷诺数的变化

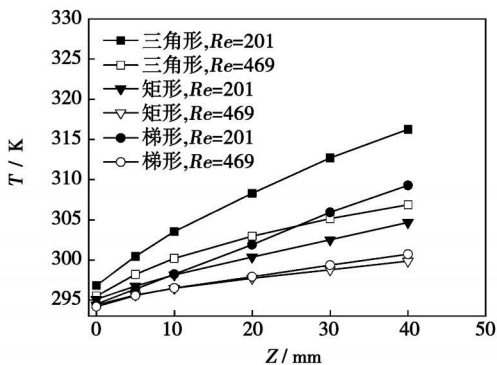


图 10 硅片下表面温度沿轴向随雷诺数的变化

图 11 给出了不同雷诺数下 3 种截面微通道中 Poiseuille 数  $fRe$  的变化趋势。从图中可以看出,  $fRe$  基本保持定值, 即  $fRe$  大小与雷诺数无关, 这与常规通道的结论相同<sup>[9]</sup>, 其中  $fRe$  定义为:

$$fRe = \frac{\Delta p \cdot d_h^2}{2 \rho \omega L} \quad (16)$$

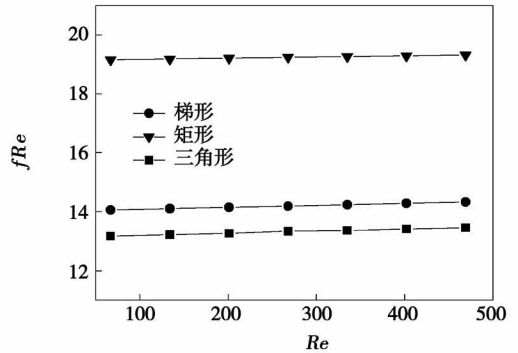


图 11 3 种截面微通道中  $fRe$  数随  $Re$  的变化趋势

### 2.3 热有效性分析

热有效性是评价热沉工作经济性的直接指标, 其定义为:

$$\eta_{\text{eff}} = \frac{Q}{P} = \frac{Q}{q_v \times \Delta p} \quad (17)$$

在相同换热量情况下, 泵功越小, 热有效性就越高。图 12 则为各流量下所耗泵功, 由图可见, 在相同流量下, 三角形通道所耗泵功最小, 热有效性最高, 梯形次之, 矩形最低。且随流量的增加, 泵功大幅度增加, 热有效性也随之大幅度降低。

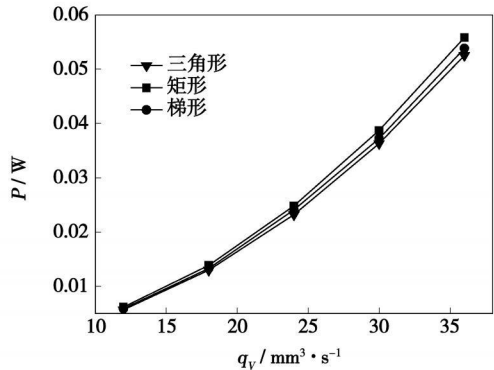


图 12 不同流量下微通道所耗泵功

## 3 结论

建立了三角形、矩形和梯形微通道内流动换热的三维模型, 并进行了数值求解, 给出了  $Nu$  数、温度和  $fRe$  数等参数的变化趋势, 并对雷诺数的影响

进行了讨论。研究发现,截面平均努塞尔数在通道入口处出现最大值,当流动充分发展时趋于恒定;流体和固体温度皆沿流动方向逐渐升高;换热面壁温仅沿流动方向近似线性升高,在垂直于流动方向,温度基本保持均衡; $Re$ 数越大,则 $Nu$ 数越大。通过热经济性比较,发现三角形通道热沉的热经济性最高。还将数值计算结果与现有实验数据进行了比较,结果显示,采用的数值模型是可靠合理的。

#### 参考文献:

- [1] TUCKERMAN D B, PEASE R F W. High-performance heat sinking for VLSI [J]. IEEE Electron Dev Lett, 1981, ELD-2(5): 126-129.
- [2] PENG X F, PETERSON G P. Convective heat transfer and flow friction for water flow in microchannel structures [J]. Int J Heat Mass Transfer, 1996, 39(12): 2599-2608
- [3] LI Z X, DU D X, GUO Z Y. Experimental study on flow characteristics of liquid in circular microtubes [J]. Microscale Thermophysical Engi-

neering, 2003 7(3): 253-265.

- [4] WU H Y, CHENG P. An experimental study of convective heat transfer in silicon microchannels with different surface conditions [J]. Int J Heat Mass Transfer, 2003, 46(14): 2547-2556.
- [5] QU W L, MAIA G M, LI D Q. Heat transfer for water flow in trapezoidal silicon microchannels [J]. Int J Heat Mass Transfer, 2000, 43(21): 3925-3936
- [6] WU H Y, CHENG P. Friction factors in smooth trapezoidal silicon microchannels with different aspect ratios [J]. Int J Heat Mass Transfer, 2003, 46(14): 2519-2525.
- [7] QU W L, MUDAWAR I. Analysis of three-dimensional heat transfer in micro-channel heat sinks [J]. Int J Heat and Mass Transfer, 2002, 45(19): 3973-3985
- [8] LI Z, TAO W Q, HE Y L. A numerical study of laminar convective heat transfer in microchannel with non-circular cross section [J]. Int J Thermal Sci, 2006, 45(12): 1140-1148.
- [9] 杨世铭, 陶文铨. 传热学 [M]. 北京: 高等教育出版社, 2006.

(编辑 滨)

#### 新技术、新产品

## 紧凑型低成本的气化器

据《Gas Turbine World》2008年1~2月号报道,为了降低IGCC(整体煤气化联合循环)设备的费用和电力生产的成本,DOE(美国能源部)和工业制造者正把减少设备费用、改进性能的先进燃气轮机和气化技术的设计研制作为目标。

在气化领域内,PWR(Pratt & Whitney Rock-etyne)已将研制火箭推进发动机的经验应用到研制一种紧凑的“低成本”气化器,用于一般的气化以及IGCC应用。

成本:项目工程师估计有潜力使气化器的成本比当前的设计减少50%。

效率:工程研究表明,可以比当今的IGCC装置的净效率提高3%。

电力成本:经济性研究表明,可以比目前的IGCC技术的电力成本降低15%~18%。

得到DOE支持正在开发的关键技术包括干给料输送泵(以便消除对费用大的联锁漏斗的需要)、先进的气化器炉衬(以便减轻耐火材料问题)和基于火箭发动机经验的新颖迅速混合的给料喷嘴。

PWR紧凑的高温气化器煤粉被泵到高压漏斗并通过一组密集相多单元冲击喷嘴。这些喷嘴给气化器供料,用于迅速燃烧的气化过程。在进入用于除去飞灰的商业用旋风分离器和棒式过滤器前,未处理的合成气经过快速的水雾急冷到约371℃,然后在被输送到燃气轮机燃烧系统前,合成气被供到脱硫过程。

(吉桂明 供稿)

long, DIAO Cheng-dong, WU Mao-song, et al (College of Energy Source and Mechanical Engineering, Northeast University of Electric Power, Jilin, China, Post Code: 132012) // Journal of Engineering for Thermal Energy & Power. — 2008, 23(6). — 630 ~ 634

By adopting a method of high-speed video camera shooting, a study has been conducted of the vortex shedding characteristics of a staggered tube bundle, which is swept across by a vertically rising gas-liquid two-phase flow in a rectangular duct. The tube bundle has been arranged in three kinds of rotating square with a pitch ratio of 1.0, 1.5 and 2.0 respectively. Shown are the whole process of entrainment of surrounding bubbles and the formation of a gas nucleus after a gas column during a vortex formation and development course. It has been concluded through a statistics survey of the vortex shedding cycles that with an increase of the void fraction within the range of the present experiment, the shedding frequency will gradually increase, leading to a shedding of the vortex, and the Strouha number assumes a gradual decrease. When the void fraction  $\alpha=0.147$ , the phenomenon of a periodical vortex shedding will eventually disappear. **Key words:** gas-liquid two phase flow, vortex shedding, staggered tube bundle

C 型混沌结构中传热强化的数值分析 = **Numerical Analysis of the Heat Transfer Intensification in a C Type Chaotic Structure** [刊, 汉] / WANG Yong-qing, DONG Qi-wu (College of Mechanical and Power Engineering, East China University of Science and Technology, Shanghai, China, Post Code: 200237), LIU Min-shan (Henan Provincial Key Laboratory on Process Heat Transfer and Energy Savings, Zhengzhou University, Zhengzhou, Post Code: 450002) // Journal of Engineering for Thermal Energy & Power. — 2008, 23(6). — 635 ~ 639

With more and more academics giving priority to and engaging in the research on intensified heat transfer, the new technology of utilizing a chaotic convection to intensify heat transfer has attracted ever increasing attention. The authors have conducted a numerical simulation of the fluid flow and heat transfer in a C-type chaotic structure by using CFD (Computational Fluid Dynamics) software Fluent, and compared the detailed information depicting the difference between the structure in question and ordinary straight structures in respect of fluid flow field distribution, temperature profile and heat transfer characteristics. Also analyzed were the intensified heat transfer performance and specific features of the C-type chaotic structure. The analytic results show that the latter enables the fluid to produce a chaotic convection at a relatively low speed. This fluid state will intensify the turbulence and perturbation of the fluid, enhance the mixing of flows in the main flow zone or at places near walls, intensify the heat transfer in flow passages, and impart a uniform temperature distribution on flow channel cross section. Moreover, the Nusselt and Poiseuille number (i. e.  $fRe$  value) for the heat transfer in a chaotic convection is no longer a constant like that of an ordinary laminar flow, but will increase with an increase of Reynolds number. **Key words:** chaotic convection, heat transfer intensification, laminar flow, computational fluid dynamics (CFD)

非圆形微通道热沉的流动换热特性数值模拟 = **Numerical Simulation of the Heat Exchange Characteristics of the Flow in a Noncircular Microchannel Heat Sink** [刊, 汉] / XIAO Chun-mei, CHEN Yong-ping, SHI Ming-heng, et al (College of Energy Source and Environment, Southeast University, Nanjing, China, Post Code: 210096) // Journal of Engineering for Thermal Energy & Power. — 2008, 23(6). — 640 ~ 644

Established was a three-dimensional model for a single-phase flow and heat exchange process in a noncircular silicon microchannel, and numerically simulated was the heat exchange of flows in a triangular, rectangular and trapezoidal microchannel respectively. It has been found that cross-sectional averaged Nusselt number attains a maximum value at the inlet of the channel, and then will drastically decrease along a fluid flow direction. It tends to be constant when the flow has been fully developed. Both solid and fluid temperatures grow in an approximately linear way along the flow direction. The wall temperatures on the heat exchange surfaces increase only along the flow direction and those along the direction perpendicular to the flow, however, basically maintain an equilibrium state. Reynolds number exercises a relatively big influence on the flow and heat exchange characteristics of the microchannel. The higher the Reynolds number, the greater the corresponding Nusselt number. It has been found through the analysis and comparison of the thermodynamic cost-effective-

ness of three kinds of microchannels that the triangular channel enjoys a maximal thermodynamic effectiveness. **Key words:** microchannel, numerical simulation, heat transfer

石化污泥与煤混烧的流化床多环芳烃排放特性 = PAH (Polycyclic Aromatic Hydrocarbon) Emission Characteristics of a Circulating Fluidized Bed Burning a Mixture of Petrochemical Sludge and Coal [刊, 汉] / ZHU Ge, ZHAO Chang-sui, LI Yong-wang, et al (Education Ministry Key Laboratory on Clean Coal Power Generation and Combustion Technology, Southeast University, Nanjing, China, Post Code: 210096) // Journal of Engineering for Thermal Energy & Power. — 2008, 23(6). — 645 ~ 648

A systematic experimental study has been conducted of the PAH (Polycyclic Aromatic Hydrocarbon) emission characteristics of a circulating fluidized bed (CFB) burning a mixture of petrochemical sludge and coal. The test was performed on a CFB test device with a dense-phase zone whose cross section is  $0.23\text{ m} \times 0.23\text{ m}$  and whose height is 7 m. It has been found that the PAH content of the sludge is far higher than that of coal. With an increase of the secondary air flow rate, the emissions of PAH from flue gas, fly ash and bottom slag show a conspicuous descending tendency. When excess air coefficient increases, PAH emission level will first go down and then up. An addition of lime stone can effectively suppress the generation of PAH. In case of an increase of Ca/S molar ratio, the emission level of the PAH will dramatically decrease. The emissions of PAH of lower molecular weight (LMW) predominate in various operating conditions. The emission amount of PAH from flying ash is way above that from the bottom slag. **Key words:** petrochemical sludge, circulating fluidized bed, hybrid combustion, polycyclic aromatic hydrocarbon (PAH)

1100 t/h 塔式炉水冷壁热负荷及变形趋势的数值模拟 = Numerical Simulation of the Thermal Load and Deformation Tendency of a 1100 t/h Tower Furnace Water Wall [刊, 汉] / DONG Chen, ZHOU Qu-lan, XU Tong-mo (College of Energy Source and Power Engineering, Xi'an Jiaotong University, Xi'an, China, Post Code: 710049), DOU Wen-yu (China Special Equipment Inspection Research Institute, Beijing, China, Post Code: 100013) // Journal of Engineering for Thermal Energy & Power. — 2008, 23(6). — 649 ~ 654

By using a self-developed numerical simulation software, a numerical simulation was conducted of the hot-state aerodynamic field and combustion process in boiler No. 1 of Pucheng Power Plant. Moreover, the problem of water wall fracture tendency was explored proceeding from the distribution of water wall thermal loads. The numerical simulation results show that when the jet flow from burner nozzles rotates spirally upward, the furnace flame center will be located excessively high and the temperature deviation at the furnace outlet is comparatively big. When the jet flow from the burner nozzles rotates spirally downward, the furnace flame center will be located at the lower part of the furnace, and the furnace temperature distribution exhibits a relatively good uniformity. The thermal loads of the walls at four sides of the furnace have a very big difference, and the water wall has an uneven thermal expansion at the four corners, thus leading to a relatively big fracture tendency. After the rotating direction of the jet flow from the burner nozzles has been adjusted from upward to downward, the thermal load deviation between the wall surfaces will decrease and the possibility of any water wall fracture diminish. In addition, the thermal load deviation of each furnace wall itself is also very big. If hydrodynamic operating conditions deteriorate, a water-wall deformation may also result. **Key words:** swirling burner, numerical simulation, wall-surface thermal load, water wall fracture

复合喷动流态化烟气脱硫工艺中一级气液区段脱硫特性研究 = A Study of Desulfurization Characteristics of a First-grade Gas-liquid Section in the Process of Compound-sprouted Fluidized Flue-gas Desulfurization [刊, 汉] / GAO Ji-lu, GAO Ji-hui, CHEN Xiao-li, et al (Combustion Engineering Research Institute, Harbin Institute of Technology, Harbin, China, Post Code: 150001) // Journal of Engineering for Thermal Energy & Power. — 2008, 23(6). — 655 ~ 660

The authors have presented a novel semi-dry-method of flue-gas purification process and conducted an experimental study of the desulfurization characteristics of a first-grade gas-liquid main reaction section in the above process by employing a